STRUCTURE, PHASE TRANSFORMATIONS, AND DIFFUSION

Kinetics of Hydrogen-Induced Forward and Reverse Diffusional Phase Transformations in an $R_2Fe_{14}B$ Hard Magnetic Alloy

V. A. Gol'tsov*, S. B. Rybalka*, A. F. Volkov*, V. V. Subbotin**, and Yu. G. Putilov**

* Donetsk State Technical University, ul. Artema 58, Donetsk, 340000
** Expromag OOO, ul. Besedova 29, Dneprodzerzhinsk, 322611

Received January 21, 1999

Abstract—The kinetics of hydrogen-induced forward and reverse phase transformations in a commercial $R_2Fe_{14}B$ alloy was studied. The isothermal kinetic curves of these transformations at temperatures from 760 to 690°C and a hydrogen pressure of 0.15 MPa were measured. Isothermal transformation diagrams of the forward and reverse phase transformations were plotted. The diagrams obtained are identical to the transformation diagrams of steels upon heating. The phase transformations studied are diffusion-controlled and proceed by the nucleation-and-growth mechanism.

INTRODUCTION

The investigation of phase transformations has always been an important part of materials science. This is confirmed by the development of hydrogen treatment as a new field of materials science [1, 2]. For example, the recently developed [3–6] HDDR process (Hydrogenation–Decomposition–Desorption–Recombination) is based on hydrogen-induced forward and reverse phase transformations in intermetallic compounds of the $R_2Fe_{14}B$ type, where R = Pr, Nd, Sm, Tb, and other rare-earth elements. The intermetallic compounds of this type are high-coercivity ferromagnetic materials currently used in the production of power compact permanent magnets [7]. A characteristic feature of these alloys is the fact that upon hydrogenation they lose their thermodynamical stability and, at elevated temperatures of 600–900°C, undergo a phase transformation, namely, diffusional decomposition into a hydride of the rare-earth component RH_x, an α-phase of Fe, and the iron boride Fe_2B [3]. Hydrogen evacuation causes the reverse phase transformation with the formation of the initial $R_2Fe_{14}B$ phase. This hydrogen treatment results in a significant grain refinement and an increase in the coercive force of the intermetallic compound. This type of hydrogen treatment, called the HDDR process, enables obtaining high-coercivity materials with H_c up to 800 kA/m. Isotropic bonded magnets produced by this technique exhibit a maximum energy product $(BH)_{max}$ of about 80 kJ/m³ [4].

Thus, the HDDR treatment of the $R_2Fe_{14}B$-type alloys is based on the hydrogen-induced forward and reverse phase transformations. The kinetics of these phase transformation has not been adequately investigated to date. So, the purpose of this work was to study the kinetics of the hydrogen-induced forward and reverse phase transformations in a commercial alloy of the $R_2Fe_{14}B$ type under isothermal and isobaric conditions, plot isothermal transformation diagrams, and analyze the specific features of this type of phase transformations.

EXPERIMENTAL

A commercial alloy of the $R_2Fe_{14}B$ type (analog of $Nd_2Fe_{14}B$ alloys) was the subject of this study. Its chemical composition (wt %) was: 36.4 R, 62.45 Fe, and 1.15 B, where R = 32% Nd + Pr and 4.4% middle and heavy rare-earth metals. The alloy was obtained from the semiproducts of a rare-earth metallic concentrate processed by a special technique.

A vacuum–hydrogen apparatus, which allows treatment in hydrogen (up to 0.2 MPa) and in vacuum (up to 10^{-2} Torr) at temperatures up to 800°C, was specially designed for the investigation of the kinetics of the phase transformations (decomposition). The procedure of detecting the new phases (α-Fe and the iron boride) formed during the phase decomposition is based on the fact that the $R_2Fe_{14}B$ alloy at the test temperatures is a paramagnetic material, while both α-Fe and the iron boride are ferromagnetic. This allows for their nucleation and growth to be detected by the magnetometric method. The measuring unit of the experimental apparatus is similar to Sadikov's one [8], conventionally used to study the kinetics of phase transformations in steels.

The following procedure was used for the investigation of the forward phase transformations. Particles of the $R_2Fe_{14}B$ alloy (0.1–1.2 mm in size and 1.017 g in weight) were placed into the working chamber, which was evacuated to 10^{-2} Torr. The samples were heated under continuous evacuation at an average rate of
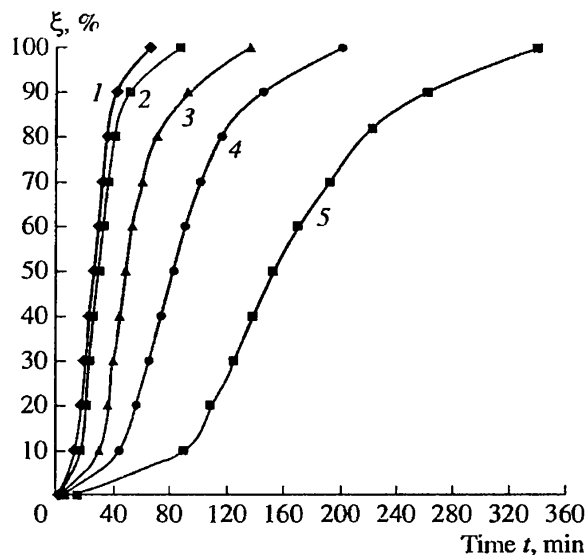
Fig. 1. Degree of the forward phase transformation ξ as a function of isothermal exposure time in hydrogen at temperatures: (1) 760; (2) 750; (3) 730; (4) 710; and (5) 690°C.
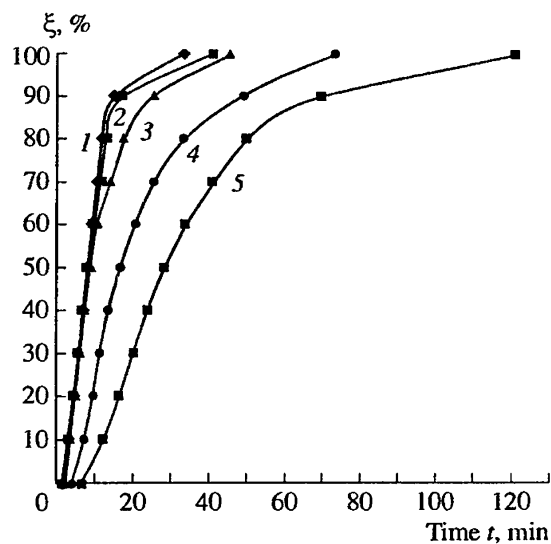

Fig. 2. Degree of the reverse phase transformation ξ as a function of isothermal exposure time in hydrogen at temperatures: (1) 760; (2) 750; (3) 730; (4) 710; and (5) 690°C.

20 K/min to a desired temperature chosen from the range of 690 to 760°C. After the establishment of isothermal conditions in the working chamber, it was filled with hydrogen to a pressure of 0.15 MPa. The forward phase transformation during the isothermal annealing was monitored by an increase in the amount of the ferromagnetic phases (α-Fe and the iron boride). After the forward phase transformation had been completed, hydrogen was gradually evacuated from the working chamber without changing the temperature. From this time, the reverse phase transformation was monitored by a decrease in the amount of the ferromagnetic phases (α-Fe and the iron boride). The data obtained were used to plot isothermal transformation diagrams of the forward and reverse phase transformations.

RESULTS AND DISCUSSION

Figure 1 shows the isothermal kinetic curves of the hydrogen-induced forward phase transformation in the commercial $R_2Fe_{14}B$ alloy at temperatures $T = 760$, 750, 730, 710, and 690°C and a hydrogen pressure of 0.15 MPa. At 760°C (Fig. 1, curve 1) the phase transformation is completed very quickly (in 65 min). A decrease in the temperature of the isothermal exposure to 750°C (curve 2) significantly slows down the phase transformation, and it is completed in 85 min. At 730°C (curve 3) and 710°C (curve 4), the phase transformation is completed in 135 and 200 min, respectively. A further decrease of the temperature causes an even greater slowdown of the phase transformation. At 690°C (curve 5), the forward phase transformation is completed in 340 min. It should be emphasized that at all temperatures there is a distinct induction period pre-

ceding the development of the phase transformation, which is detected by the first signs of the formation or disappearance of the ferromagnetic phases. The incubation period varies from 3 min at 760°C to 15 min at 690°C, i.e., the decrease in the temperature of the isothermal exposure by only 70 K (from 760°C to 690°C) causes a significant (about fivefold) increase in the incubation period.

The results of the kinetic study of the reverse phase transformation are generalized in Fig. 2. The phase transformation at 760°C (Fig. 2, curve 1) is completed in 33 min. At temperatures of 750°C (curve 2) and 730°C (curve 3), the phase transformation is completed in 40 and 45 min, respectively. A further decrease in the temperature of the isothermal exposure causes a greater slowdown of the reverse phase transformation. At 710°C (curve 4), the phase transformation is completed in 72.5 min. At 690°C (curve 5), it requires 120 min to complete the reverse phase transformation.

In the case of the reverse phase transformation, the tendency of the increase in the induction period with the decrease in the temperature of isothermal exposure is retained. The induction period varies from 1.25 min at 760°C to 6.5 min at 690°C. Note that the reverse phase transformation, as compared with the forward one, is characterized by significantly higher transformation rates (approximately by two to three times) and lower induction periods (approximately by two to three times).

Now, let us consider the results in terms of the mechanisms of phase transformations. The forward hydrogen-induced phase transformations of the type at hand (studied most thoroughly for the $Nd_2Fe_{14}B$ alloy)
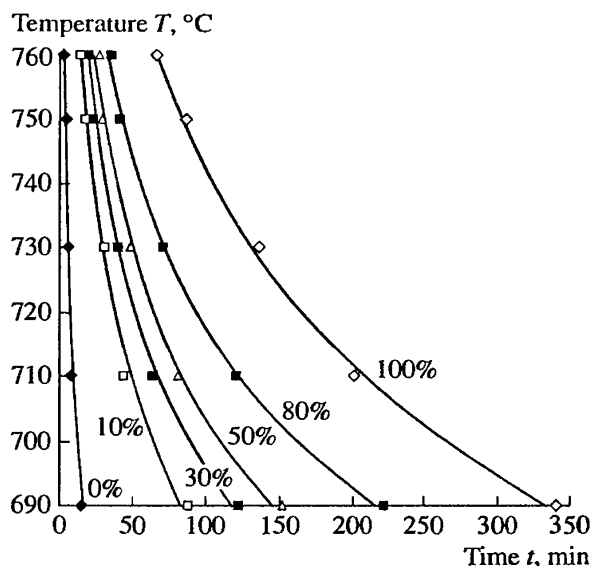
Fig. 3. Isothermal transformation diagram of the forward phase transformation in the $R_2Fe_{14}B$ alloy at a hydrogen pressure of 0.15 MPa.
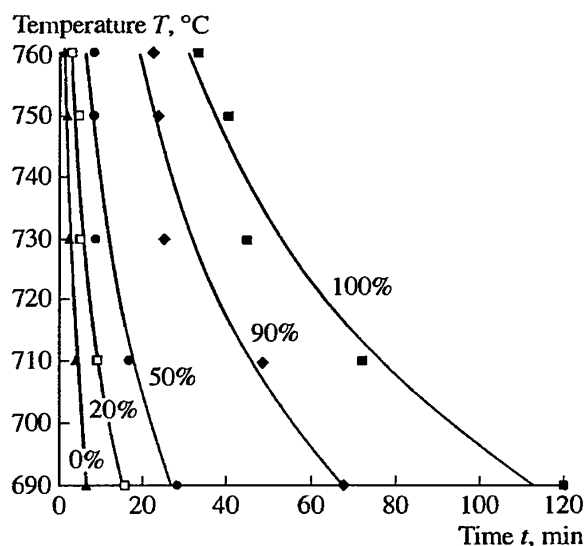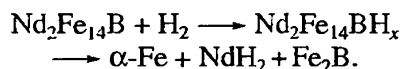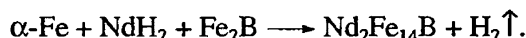

Fig. 4. Isothermal transformation diagram of the reverse phase transformation in the $R_2Fe_{14}B$ alloy in a vacuum of $\sim 10^{-2}$ Torr.

proceed in a hydrogen atmosphere according to the following scheme [4]:

$$Nd_2Fe_{14}B + H_2 \longrightarrow Nd_2Fe_{14}BH_x$$
$$\longrightarrow \alpha\text{-Fe} + NdH_2 + Fe_2B.$$

The reverse phase transformations in a vacuum proceed, according to [4], the scheme

$$\alpha\text{-Fe} + NdH_2 + Fe_2B \longrightarrow Nd_2Fe_{14}B + H_2\uparrow.$$

It is obvious that the phase transformations of this type require a diffusion transfer of atoms of the components (Nd, Fe, B) of the intermetallic compound. Note that two types of diffusional phase transformations are known, namely: spinodal decomposition, and transformations that occur via the normal mechanism of nucleation and growth.

Phase transformations that occur via the spinodal decomposition mechanism require very small-distance diffusional displacements of the alloy components and, therefore, may proceed at rather low temperatures and at relatively high rates. The phase transformations proceeding through the nucleation-and-growth mechanism require large-distance (as compared with interatomic spacing) diffusion of atoms of the components and, therefore, occur at relatively high temperatures and need more time to be completed. As is seen from Figs. 1 and 2, the behavior of the isothermal transformation diagrams (with a gradual decrease in the phase transformation rate and the presence of a distinctive induction period and its dependence on temperature) indicate that the phase transformations under study proceed by the nucleation-and-growth mechanism. Phase transformations by the nucleation-and-growth mechanism are known [9] (as has been most thoroughly inves-

tigated for steels) to exhibit two types of isothermal transformation diagrams. C-shaped curves occur in those cases where, with decreasing temperature and increasing undercooling below the critical point of the phase transformation, first the increase in the new-phase-nucleation rate and then the diffusion retardation of the phase transformation are prevailing.

Phase transformations of the other type (e.g., transformations in steels upon heating) have a different type of isothermal transformation diagram. In this case, both factors act in the same direction and, therefore, the phase transformation accelerates as the temperature increases.

Figures 3 and 4 display isothermal transformation diagrams of the forward and reverse hydrogen-induced phase transformations in the $R_2Fe_{14}B$ intermetallic compound plotted from the data of Figs. 1 and 2. Both the forward and reverse phase transformations are seen to yield isothermal transformation diagrams of the second type. The diffusivities of Nd, Fe, and B atoms are undoubtedly increasing with temperature, but the approximately fivefold acceleration of the phase transformation within a narrow temperature range (70 K) from 690 to 760°C can hardly be explained by the increase in the diffusivities only (even with allowance for a drastic acceleration of diffusion in solids due to hydrogen). The principal factor is likely to be a drastic increase in the nucleation rate of the new phases with increasing temperature, but this requires a more detailed investigation.

For further analysis of the phase transformation mechanism, we used the phenomenological theory of
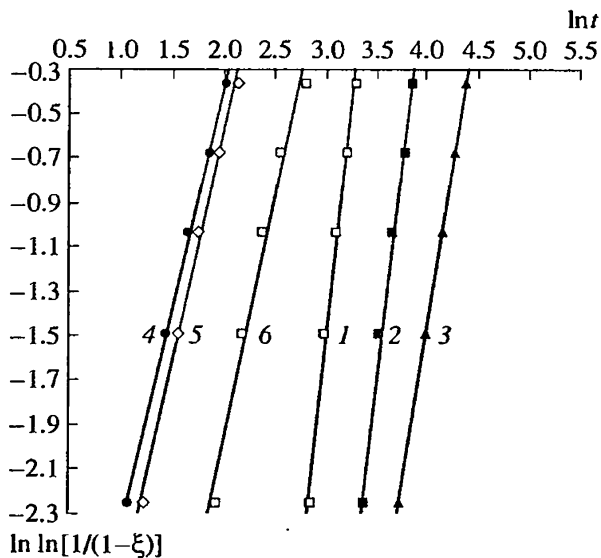
Fig. 5. Avrami curves at various temperatures of the isothermal exposure for the forward (*1–3*) and reverse (*4–6*) phase transformations: (*1*) 750; (*2*) 730; (*3*) 710; (*4*) 750; (*5*) 730; (*6*) 710°C.

Avrami [10], according to which the degree of phase transformation ξ is expressed as

$$\xi = 1 - \exp(-kt^n),$$

where *t* is the time, and *k* and *n* are constants.

Plots of the experimental results in the lnln[1/(1 − ξ)] vs. ln*t* axes (Fig. 5) show linear behavior. The slopes of the lines give the average values $n = 3.9$ for the forward phase transformation and $n = 2.3$ for the reverse transformation. According to the Avrami theory, if $1 < n < 4.0$, the phase transformation occurs via the nucleation-and-growth mechanism with a diffusion-controlled growth rate of nuclei of the new phase. Hence, the forward and reverse phase transformations under study can be identified as hydrogen-induced diffusional phase transformations.

CONCLUSIONS

(1) The kinetics of hydrogen-induced forward and reverse phase transformations in a $R_2Fe_{14}B$-type alloy was studied. The rates of the reverse phase transformation were shown to be two to three times higher than those of the forward transformations. The decrease in the temperature of the isothermal phase transformation from 760 to 690°C was found to cause a dramatic (approximately fivefold) slowdown of both the forward and reverse phase transformations. The phase transfor-

mations studied were characterized by an induction period increasing with decreasing temperature of the isothermal phase transformation.

(2) The isothermal transformation diagrams of the forward and reverse phase transformations were found to be similar to the isothermal transformation diagrams of steels subjected to continuous heating. This indicates a drastic increase in the nucleation rate of the new phases with increasing temperature.

(3) The phase transformations studied are well described by the Avrami phenomenological theory of phase transformations. They are diffusion-controlled phase transformations that proceed by the nucleation-and-growth mechanism.

REFERENCES

1. Goltsov, V.A., History, Ideology and Prospects of the Hydrogen Treatment of Materials—Opening Address, *Int. J. Hydrogen Energy*, 1997, vol. 22, nos. 2/3, pp. 115–117.
2. Goltsov, V.A., Fundamentals of Hydrogen Treatment of Materials and Its Classification, *Int. J. Hydrogen Energy*, 1997, vol. 22, nos. 2/3, pp. 119–124.
3. Takeshita, T., Present Status of the Hydrogenation–Decomposition–Desorption–Recombination Process as Applied to the Production of Magnets, *J. Alloys Compd.*, 1993, vol. 193, pp. 231–234.
4. Takeshita, T., Some Applications of Hydrogenation–Decomposition–Desorption–Recombination (HDDR) and Hydrogen–Decrepitation (HD) in Metals Processing, *J. Alloys Compd.*, 1995, vol. 231, pp. 51–59.
5. Ragg, O.M., Keegan, G., Nagel, H., and Harris, I.R., The HD and HDDR Processes in the Production of Nd–Fe–B Permanent Magnets, *Int. J. Hydrogen Energy*, 1997, vol. 22, nos. 2/3, pp. 333–342.
6. Fruchar, D., Bacmann, M., de Rango, P., Ishard, O., Liesert, S., Miraglia, S., Obbade, S., Soubeyroux, J.-L., Tomey, E., and Wolfers, P., Hydrogen in Hard Magnetic Materials, *J. Alloys Compd.*, 1997, vols. 253–254, pp. 121–127.
7. Mishin, D.D., *Magnitnye materialy* (Magnetic Materials), Moscow: Vysshaya Shkola, 1991.
8. Livshits, B.G., *Fizicheskie svoistva chernykh metallov i metody ikh ispytanii* (Physical Properties of Ferrous Metals and Methods of Their Tests), Moscow: Otd. Nauchn. Tekh. Inform., 1937.
9. Popova, L.E. and Popov A.A., *Diagrammy austenitnykh prevrashchenii v stalyakh i β-rastvorov v titanovykh splavakh* (Diagrams of Austenite Transformations in Steels and β Solid Solutions in Titanium Alloys), Moscow: Metallurgiya, 1993.
10. Christian, J., *The Theory of Transformations in Metals and Alloys, part 1: Equilibrium and General Kinetic Theory*, Oxford: Pergamon, 1975.